

## Improved determination of the astrophysical $S(0)$ factor of the $^{15}\text{N}(p, \alpha)^{12}\text{C}$ reaction

M. La Cognata,<sup>1</sup> V. Z. Goldberg,<sup>2</sup> A. M. Mukhamedzhanov,<sup>2</sup> C. Spitaleri,<sup>1,\*</sup> and R. E. Tribble<sup>2</sup>

<sup>1</sup>DMFCI, Università di Catania, Catania, Italy and INFN-Laboratori Nazionali del Sud, Catania, Italy

<sup>2</sup>Cyclotron Institute, Texas A&M University, College Station, Texas 77843, USA

(Received 13 April 2009; revised manuscript received 27 May 2009; published 13 July 2009)

We present new improved  $R$  matrix fits of direct data and indirect Trojan Horse data for the  $^{15}\text{N}(p, \alpha)^{12}\text{C}$  reaction and provide a more accurate recommended value of  $S(0) = 73.0 \pm 5.0$  MeV b from direct Redder data [A. Redder *et al.*, *Z. Phys. A* **305**, 325 (1982)] and  $S(0) = 70.0 \pm 13.5$  MeV b from the Trojan Horse data [M. La Cognata *et al.*, *Phys. Rev. C* **76**, 065804 (2007)]. We also analyze a recent fit by Barker [F. C. Barker, *Phys. Rev. C* **78**, 044611 (2008)] and demonstrate that when all the uncertainties are taken into account, our results overlap with his. We also provide a fit of the Trojan Horse data that properly takes into account finite residual energy resolution of the data.

DOI: [10.1103/PhysRevC.80.012801](https://doi.org/10.1103/PhysRevC.80.012801)

PACS number(s): 24.10.-i, 26.20.-f, 25.40.Hs, 27.20.+n

$^{15}\text{N}(p, \alpha)^{12}\text{C}$  is an important carbon-nitrogen-oxygen cycle reaction and plays a crucial role in the production chain of the key isotope  $^{19}\text{F}$  in asymptotic giant branch stars. Because of its astrophysical relevance (see Ref. [1] and reference therein) it has been subject to both direct [2–4] and indirect [via the Trojan Horse method (THM)] [1] investigations to extend our knowledge down to the Gamow window. Recently Barker presented new  $R$  matrix fits [5] to the direct measurements of this reaction by Zyskind and Parker [2] and Redder [4]. In making fits, Barker used two different sets of data from Ref. [4], one that included the full 71 data points (R71), and one that used the lowest energy data (R32). He also fit the recent indirect measurement via the THM [1]. The  $R$  matrix fit by Barker [5] to the direct data yields  $S(0) \approx 80$  MeV b, which is above the values recommended by all other publications except for the result from Ref. [2], which has a 15% systematic and 8% statistical uncertainty. In Fig. 1, the  $S(0)$  factors obtained by extrapolation of direct measurements [2–4] are compared with the measured indirect value [1] and the full  $R$  matrix extrapolation [5], and with the recommended values in the most recent compilations, namely, NACRE [6] and Adelberger *et al.* [7]. Figure 1 demonstrates that all the experimental values are in agreement with each other within the experimental uncertainties, resulting in  $S(0) \approx 62$  [3],  $S(0) = 78 \pm 13$  [2],  $S(0) = 65 \pm 4.0$  [4], and  $S(0) = 68 \pm 11$  MeV b [1]. The compilations by NACRE [6] and Adelberger *et al.* [7] recommended  $S(0) = 65 \pm 7$  and  $S(0) = 67.5 \pm 4.0$  MeV b, correspondingly, relying on the results from Ref. [4]. Here we address the analysis of the data and  $R$  matrix fit in Ref. [5] with a recommended value for  $S(0)$ . We present a new  $R$  matrix fit of the THM data taking into account the residual energy resolution, which provides results in agreement with those in the literature. The effect of the final energy resolution was not included in the fit of the THM data in Ref. [5].

In Fig. 2, we show our best two-level, two-channel  $R$  matrix fits to the R71 (solid blue line) and R32 data (dashed red line) leading to  $S(0) = 74 \pm 9$  and  $S(0) = 73 \pm 5$  MeV b,

respectively. The uncertainties are determined by the experimental and  $R$  matrix fit uncertainties. In these fits we took into account the importance of fitting of the low-energy data aiming to obtain an accurate  $S(0)$  value. Both results agree very well. We note that our fit leads to a slightly higher value of  $S(0)$  than that obtained in Ref. [4], because we used, as in Ref. [5], the full  $R$  matrix approach rather than the Breit-Wigner expression for the interfering resonances.

Because of the very steep descent of the  $S(E)$  factor at low energies, the low-energy measurements of the  $S(E)$  factor become very critical in obtaining reliable information about  $S(0)$ . That is why the THM, the only method that allows one to measure the  $S(E)$  factor down to the Gamow peak, is imperative in the case under consideration to determine the  $S(0)$  factor. The THM reaction  $^2\text{H}(^{15}\text{N}, \alpha)^{12}\text{C}n$  has been used in Ref. [1] to determine the  $S(E)$  factor for the  $^{15}\text{N}(p, \alpha)^{12}\text{C}$  reaction down to 19 keV. The  $S(E)$  factor obtained by normalization of the THM data to the direct data from Ref. [4] at the resonance peak is shown as red dots in Fig. 3 and compared with other direct measurements. In Fig. 4, we compare the behavior of the  $S(E)$  factor determined from the THM with direct data sets within the range of relevance for astrophysics. As was stated in Ref. [1], for the first time we were able to access the low-energy region in the  $^{15}\text{N}(p, \alpha)^{12}\text{C}$  reaction by means of an experiment and measure the bare-nucleus  $S(E)$  factor.

Typically, two main issues have to be addressed in the THM application, namely, the normalization to direct data to get the absolute cross section and the estimate of the effects of the energy spread. Indeed, these two problems are strictly connected, as the energy spread changes the shape of the observed resonances, thus a suitable normalization procedure has to be devised and a careful uncertainty evaluation is required. In the  $^{15}\text{N}(p, \alpha)^{12}\text{C}$  reaction studied by means of the THM, normalization to direct data is obtained by equating the areas subtended by the resonance at 314 keV, for this resonance has been accurately measured in a previous experiment [4]. The experimentally determined energy resolution in Ref. [1] turns out to be a significant fraction of the natural width of the 314 keV peak, ranging from 20 to 80 keV (full width at half maximum), depending on the kinematic conditions. Therefore,

\*[Spitaleri@lns.infn.it](mailto:Spitaleri@lns.infn.it)

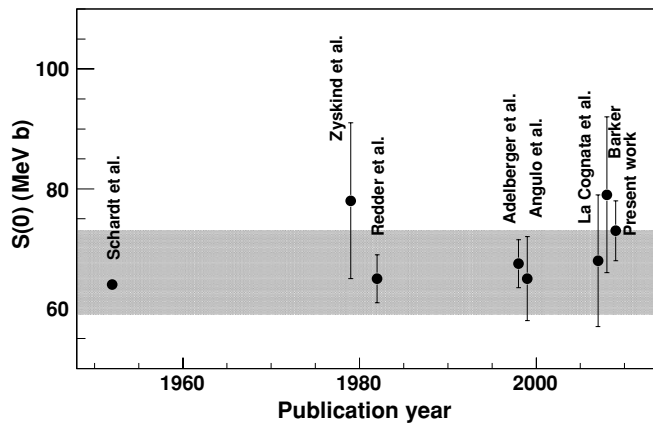


FIG. 1. Summary of the available astrophysical  $S(0)$  factors of the  $^{15}\text{N}(p, \alpha)^{12}\text{C}$  reaction.

the resonant peak is broader than the one displayed by direct data, as it represents the convolution of the original resonance shape and of the detector response; whereas the peak value is depressed in comparison to the directly measured one, to keep the area below the peak the same in both cases. To get the best estimate of the THM  $S(E)$  factor for the  $^{15}\text{N}(p, \alpha)^{12}\text{C}$  reaction in Ref. [1], a deconvolution procedure has been adopted to subtract the energy spread.

A function has been evaluated such that it reproduces the THM  $S(E)$  factor if it is smeared out by the estimated energy spread. The red dots in Fig. 3 show the THM  $S(E)$  factor obtained by the described procedure. It is the best estimate of the  $S(E)$  factor measured with an ideal resolution. Note that the experimental uncertainties (including statistical and normalization errors), the bin chosen to represent the data, and the choice of the folding function (which is a simple bell-shaped function) do not allow us to fully remove the effect

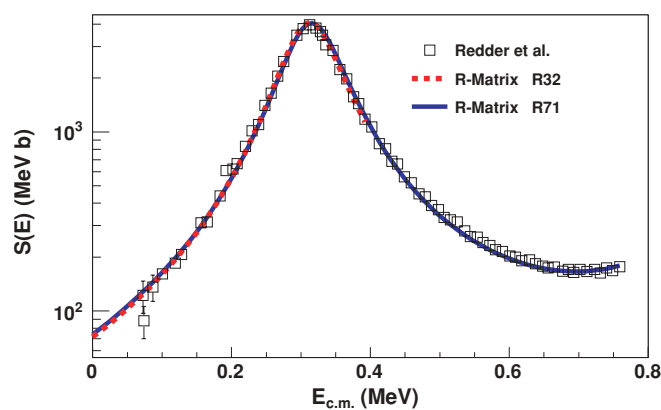


FIG. 2. (Color online) Solid blue (dashed red) line is our fit to R71 (R32) data (squares) [4], giving  $S(0) = 74$  MeV b,  $\chi^2/N = 1.47$  [ $S(0) = 73$  MeV b,  $\chi^2/N = 1.17$ ]. All the parameters are the same as in Table I of Ref. [5] for fit B for the R71 data (fit B for R32 data), except for the channel radius in the  $\alpha$  channel  $r_{0\alpha} = 7.0$  fm and  $\gamma_{1\alpha} = -0.1015$  MeV $^{1/2}$  ( $\gamma_{1\alpha} = -0.1015$  MeV $^{1/2}$  and  $\gamma_{2\alpha} = 0.083$  MeV $^{1/2}$ ). The boundary conditions are chosen so that the energy of the second level coincides with the second resonance energy [5].

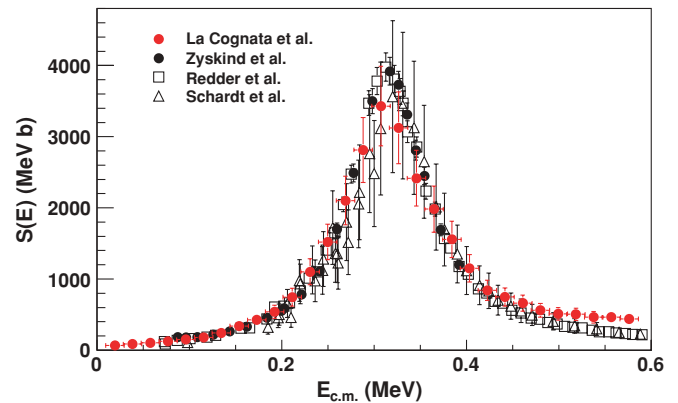


FIG. 3. (Color online) Comparison of the available experimental data of the  $^{15}\text{N}(p, \alpha)^{12}\text{C}$  reaction at astrophysical energies.

of energy resolution. That is why we refer to the best estimate of the ideal resolution  $S(E)$  factor. Indeed, the agreement is good below 400 keV, as clearly displayed in Fig. 3. However, we underscore that a perfect reproduction of the resonant structure does not represent a primary goal of this experiment, since it has been previously measured with sufficient accuracy [4]. We rather aimed to explore the low-energy region, where no experimental data are available but only extrapolations and where electron screening can play a significant role. Anyway, we underscore that the error bars affecting the THM data account for the uncertainties due to the unfolding procedure. Indeed, it turns out that they make one of the main contributions to the overall experimental uncertainties.

In Fig. 5, we show how the  $S(E)$  factor fit with ideal resolution data changes after convolution with the final energy resolution. Our  $R$  matrix fit to R71 data set (blue solid line) is chosen to represent the trend of the direct  $S(E)$  factor. To make an improved comparison of the THM and direct data, we have convoluted the  $R$  matrix  $S(E)$  factor with a 20 keV energy resolution, which is shown as a black solid line in Fig. 5 (the red dots are the THM data [1]). The convolution decreases the resonant peak value making the resonance wider but does not affect the tails. At the region above 400 keV, contributions from  $^{13}\text{C}$  sequential decay add up to the quasi-free yield [see Fig. 4(b) in Ref. [1]] leading to an increase of the

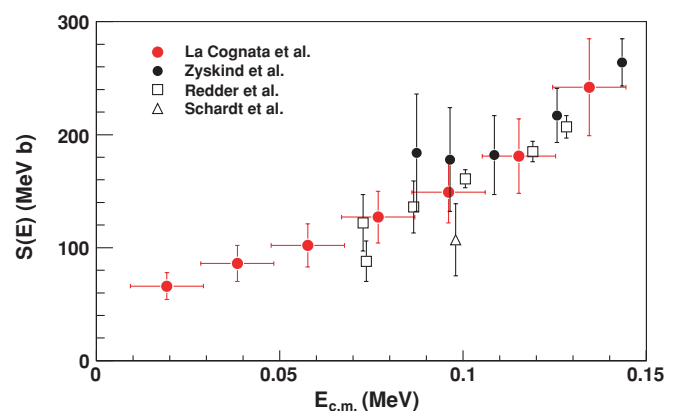


FIG. 4. (Color online) Comparison of the available experimental data of the  $^{15}\text{N}(p, \alpha)^{12}\text{C}$  reaction for  $E \leq 150$  keV.

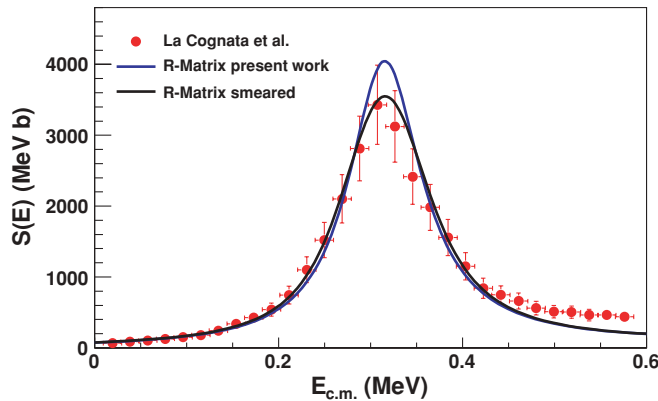


FIG. 5. (Color online) Effect of finite energy resolution on the  $S(E)$  factor. The blue solid line, which is the same as the blue solid line in Fig. 2, represents the  $S(E)$  factor obtained by fitting the direct R71 data (ideal energy resolution) [4] for the  $^{15}\text{N}(p, \alpha)^{12}\text{C}$  reaction. The black solid line is the  $S(E)$  factor obtained by folding the ideal energy resolution  $S(E)$  factor (blue solid line) with the final energy resolution of 20 keV. For comparison, the THM data (red dots) are also shown [1].

THM  $S(E)$  factor compared to the  $R$  matrix fit. The fit of the THM data using the half-off-energy-shell (HOES) Breit-Wigner equation for two interfering resonances for the channel radius  $r_0 = 5.5$  fm, gave  $S(0) = 68 \pm 11$  MeV b in Ref. [1]. These results are fully consistent with the previous direct measurements as well as with a polynomial fit of the low-energy THM data that gave  $S(0) = 62 \pm 10$  MeV b [1]. To improve our fit of the THM data, we present a full two-level, two-channel HOES new  $R$  matrix fit, in which the entry channel proton partial widths are replaced by the amplitudes of the direct transfer  $^2\text{H}(^{15}\text{N}, ^{16}\text{O})n$  reaction populating the first and second  $1^-$  resonances. The THM reaction amplitude in the presence of two interfering resonances in the compound nucleus  $F$ , which is the case for the  $^{15}\text{N}(p, \alpha)^{12}\text{C}$  reaction, takes the form (if nuclear spins are neglected) [8]

$$M^{(R)}(\mathbf{k}_{nF}, \mathbf{k}_{\alpha C}; \mathbf{k}_{dA}) = \sum_{\tau, \nu=1,2} \Gamma_{\alpha(\tau)}^{1/2}(E_{\alpha C}) [\mathbf{A}^{-1}]_{\tau\nu} M_{\nu}(\mathbf{k}_{nF}, \mathbf{k}_{dA}), \quad (1)$$

where  $\mathbf{A}$  is the level matrix,  $\Gamma_{\alpha(\tau)}(E_{\alpha C})$  is the  $\alpha$  partial width of resonance  $\tau$  in the channel  $\alpha + C$ ,  $M_{\nu}(\mathbf{k}_{nF}, \mathbf{k}_{dA})$  is the amplitude for the direct transfer reaction  $d + A \rightarrow n + F_{\tau}$  populating the compound state  $F_{\tau}$  of the system  $F = p + A = \alpha + C$ ,  $A = ^{15}\text{N}$ ,  $C = ^{12}\text{C}$ ,  $\mathbf{k}_{ij}$  is the relative momentum of particles  $i$  and  $j$ , and  $E_{ij}$  is their relative energy. Equation (1) is designed to fit an ideal energy resolution data. To reproduce the finite energy resolution THM data, we fold the  $R$  matrix  $S(E)$  factor with a residual energy resolution of 20 keV, similar to what we did to obtain the solid black line in Fig. 5. In Fig. 5, we fold the  $R$  matrix  $S(E)$  factor, which fits the direct R71 data [4], with the residual 20 keV energy resolution and demonstrate that it fits the THM data. In Fig. 6, we do the reverse: we fit the THM data using the HOES  $R$  matrix  $S(E)$  factor convoluted with the residual 20 keV energy resolution (black solid line) and demonstrate that the HOES  $R$  matrix

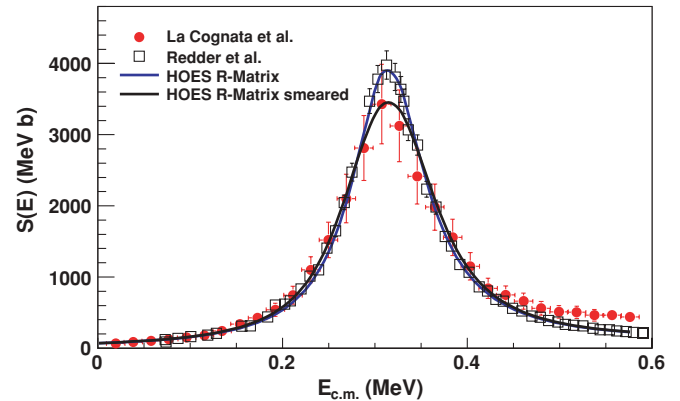


FIG. 6. (Color online) Black solid line is a 20 keV energy-resolution folded  $R$  matrix fit to THM data (red dots) [1], giving  $S(0) = 70 \pm 8$  MeV b ( $\chi^2/N = 1.16$ ), with parameters  $r_{0p} = 5.03$  fm,  $r_{0\alpha} = 7.0$  fm,  $\gamma_{21} = 0.87$ ,  $\gamma_{1p} = 0.638$  MeV $^{1/2}$ ,  $\gamma_{1\alpha} = -0.1015$  MeV $^{1/2}$ ,  $\gamma_{2p} = 0.520$  MeV $^{1/2}$ , and  $\gamma_{2\alpha} = 0.083$  MeV $^{1/2}$ . The blue solid line is the  $R$  matrix fit of the R32 data ( $\chi^2/N = 1.39$ ) obtained with the same parameters as the solid black line. For comparison, the  $S(E)$  factor from Ref. [4] is given as open squares.

$S(E)$  factor (blue solid line) simultaneously fits the direct R32 data. The THM data are normalized to the direct cross section in the energy interval from 200 to 400 keV. The HOES  $R$  matrix fit to the THM data contains a new parameter,  $\gamma_{21}$ , which is the ratio of the amplitudes for direct transfer reactions  $^{15}\text{N}(d, n)^{16}\text{O}$  populating the second ( $E_x = 13.09$  MeV) and first ( $E_x = 12.44$  MeV)  $1^-$  resonances in  $^{16}\text{O}$ . This ratio, determined from the available experimental cross sections for the corresponding transfer reactions [9], is  $\gamma_{21} \approx 0.87 \pm 0.20$ . This has the advantage that any effect connected, e.g., with isospin mixing or more generally to more complex nuclear structure is automatically taken into account. The  $R$  matrix fit to the THM data shown in Fig. 6 is performed by varying  $\gamma_{21}$  and keeping all other parameters fixed at values obtained to fit the direct R32 data (see caption to Fig. 2). It turns out that THM and direct data place a stronger constraint on the  $\gamma_{21}$  variability range than the transfer reaction data, i.e., if we assign marginal values of the ratio  $\gamma_{21}^{\min} = 0.67$  or  $\gamma_{21}^{\max} = 1.07$ , the fit is very poor, especially at low energies. We find that the best fit of the THM data is for  $0.87 \leq \gamma_{21} \leq 0.95$ . Both  $\gamma_{21} = 0.87$  and  $\gamma_{21} = 0.95$  give a similar fit to the THM data, but the first one provides a much better fit to the direct R32 data.

Figure 6 is the main result of this paper. Our calculations present compelling evidence that the THM measures the same cross section as the direct measurements. The smearing over the energy resolution affects only the maximum value of the resonance peak, keeping the resonance area the same, and it does not affect the low-energy tail. This effect was not included in the analysis carried out in Ref. [5], which led to a different result quoted there. The  $S(E)$  factor folded with 20 keV energy resolution (the black solid line in Fig. 6) is in perfect agreement with our THM data. The total uncertainty of the THM data is 16% [1]. An additional 11% comes from the  $\gamma_{21}$  uncertainty, which is caused by the transfer reaction experimental uncertainties not related to the THM reaction. Then, we estimate the total uncertainty of the THM  $S(E)$  factor

to be 19%. Thus from the THM, we get the  $S(0) = 70.0 \pm 13.5$  MeV b factor, which agrees with the direct R71 and R32 data fits. A significant part of the  $\chi^2$  for the THM data fit comes from the energy region  $E > 400$  keV, where the contribution from the non-THM mechanism, sequential decay of  $^{13}\text{C}$ , becomes significant. It means that the THM does allow one to extract information about nuclear reactions of astrophysical relevance. Meanwhile, we have verified that the modified  $R$  matrix approach correctly describes the THM  $S(E)$  factor in the case of resonant reactions. On the one hand, this provides an explanation of why the THM is working, and, on the other, it allows one to deduce a reliable  $S(0)$  factor for astrophysical application.

The present  $S(0)$  is slightly larger than what was given in Ref. [1]. This is essentially due to using here the two-level, two-channel  $R$  matrix rather than the Breit-Wigner equation for two interfering resonances used in Ref. [1]. This shows that the approximations used in Ref. [1] are justified, bearing in mind the uncertainties affecting the experimental data.

Now we compare our results with Barker's fits [5]. We note that no uncertainties of the fits are given in Ref. [5], which makes it difficult to compare with other available results. For fitting, Barker used three different data sets from direct measurements: the Zyskind and Parker (ZP) data [2] and the R71 and R32 data points [4]. In the case under consideration, because of the steep slope of the  $S(E)$  factor at low energies, an accurate determination of  $S(0)$  requires knowledge of  $S(E)$  at the lowest possible energies with small uncertainties, which makes the Redder data [4] preferable to the ZP [2]. Barker obtained a fit for the ZP data but failed to reproduce the low-energy Redder data. We remind the reader that the ZP data were measured with larger uncertainties than the Redder data at low energy, and the smallest measured energy in Ref. [2] was 87.3 keV (with only 21 data points) versus 72.7 keV reached in Ref. [4] with 71 data points. Moreover, for  $E \leq 150$  keV, the ZP data [2] display a sudden increase in the uncertainty (see Fig. 4) with the trend suggesting an increase in the  $S(E)$  factor toward lower energies, which contradicts the Redder data [4] as well as the previous data by Schardt *et al.* [3]. It is clear why Barker obtained smaller  $\chi^2$  for the fit of the ZP data,  $\chi^2 \sim 0.1$ , because of the larger uncertainties of the ZP data compared to the Redder data and the smaller fitting interval. The average result of fits A, B, and C (if the fit D is rejected because of the low  $\gamma_{2p}$  and large  $\gamma_{2\alpha}$ ) is  $S(0) = 79$  MeV b. Taking into account that the total (systematic 15% and statistical 8%) uncertainty of the ZP data [2] is 17%, we conclude that the fit in Ref. [5] is  $S(0) = 79 \pm 13$  MeV b.

In Fig. 7, we show the quality of Barker's fit to the Redder R71 data [4] following his procedure and the results given in Table I from Ref. [5]. Fit A, which significantly overestimates the low-energy experimental data, was rejected in Ref. [5] because of the high  $\chi^2$ . For fit B, which was accepted in Ref. [5], we find  $S(0) = 82$  MeV b rather than 80 MeV b reported in Ref. [5]. This fit also overestimates the low-energy data. Fit C leading to  $S(0) = 82$  MeV b is very close to fit B, which is why it is not shown in Fig. 8. To determine the sensitivity of the  $R$  matrix fit to the channel radius, we redid the fit for  $r_{0\alpha} = 7.0$  fm. The fit obtained by keeping all the parameters the same as in Ref. [5] except for  $\gamma_{1\alpha} = -0.1015$  MeV $^{1/2}$

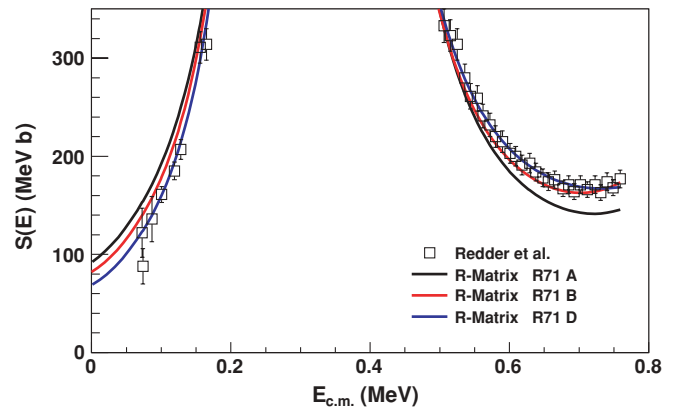


FIG. 7. (Color online) Solid black line is Barker's fit A, Table I in Ref. [5], to R71 data (black squares) [4], giving  $S(0) = 92$  MeV b; blue line is fit B, Table I, giving  $S(0) = 82$  MeV b; and the red line is fit D, Table I, giving  $S(0) = 69$  MeV b.

gave  $S(0) = 74$  MeV b with  $\chi^2 = 1.20$ , i.e., we can assign  $\approx 10\%$  uncertainty of the  $R$  matrix fit due to the ambiguity of the channel radius value. Taking also into account the experimental uncertainty in Ref. [4] of  $\sim 6\%$ , we assign  $S(0) = 82 \pm 10$  MeV b for Barker's fit of the R71 data. Definitely the best fit is R71 D, which gives  $S(0) = 69$  MeV b, but it was rejected in Ref. [5] because of the high  $\gamma_{2\alpha}$ . It is compelling evidence that the two-level  $R$  matrix fit by Barker of the R71 data, which heavily relies on higher energies ( $\gtrsim 400$  keV), does not account for higher energy levels or even a direct reaction mechanism.

Elimination of the higher energy region improves the fit. In Fig. 8, we show the fits to R32 data [4] obtained in Ref. [5]. The fits to R32 data are better in the low-energy region than the fits to R71 data, and elimination of the data at higher energies decreases the  $S(0)$  factor for fit A by 13 MeV b and for fit B by 7 MeV b, leading to  $S(0) = 79$  MeV b for the fit R32 A and 75 MeV b for the fit R32 B. Careful inspection shows that both fits to R32 data slightly overestimate the central experimental data at low energies, but fit B is definitely better. Indeed, it

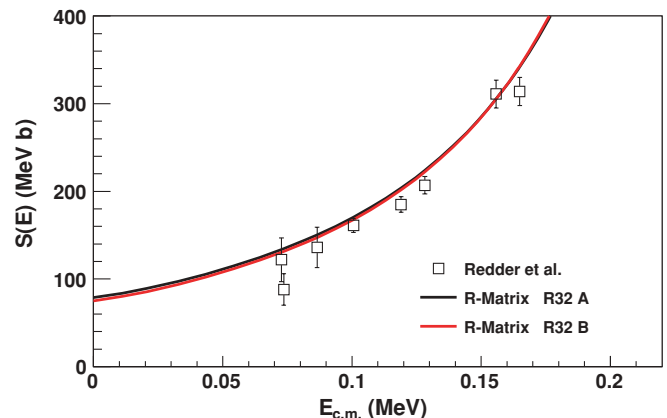


FIG. 8. (Color online) Solid black (red) line is the Barker's fit A (B), Table I [5] to R32 data (black squares) [4], giving  $S(0) = 78(74)$  MeV b.

is clear that the lower the  $S(0)$  value, the better the fit, thus strengthening the previously published results. Note that fit C to the R32 data, which is not shown, has a very similar behavior to the R32 B. Again, fit D (also not shown), which gives the best fit with  $S(0) = 56$  MeV b, was rejected due to too high a  $\gamma_{2\alpha}$  value. The fit for the R32 data with the channel radius  $r_{0\alpha} = 7.0$  fm and  $\gamma_{1\alpha} = -0.100$  MeV<sup>1/2</sup> with all other parameters kept the same as in Ref. [5] gives  $S(0) = 72$  MeV b. It contributes an additional 4% uncertainty to the  $R$  matrix fit because of the channel radius ambiguity. Then the total uncertainty for the R32 data is 8% leading to  $S(0) = 77 \pm 6$  MeV b. Taking into account all the uncertainties of our and Barker's  $R$  matrix fits to the [4] data, we can conclude that they do overlap. We have a better fit than Barker in the low-energy region and lower central value of the  $S(0)$  factor.

In the fit to our THM data presented in Ref. [5], the ratio of the amplitudes for the direct transfer  ${}^2\text{H}({}^{15}\text{N}, {}^{16}\text{O})n$  reaction populating the second and first  $1^-$  resonances is used as a fitting parameter. The ratio 1.6–1.9 obtained in Ref. [5] does not have any physical meaning. Then from

Barker's fit, it follows that the ratio of the cross sections for the direct transfer  ${}^2\text{H}({}^{15}\text{N}, {}^{16}\text{O})n$  reaction populating the second and first  $1^-$  resonances is as large as 2.6–4, which significantly contradicts the experimental value  $\lesssim 1$  for the  $(d, n)$  reaction [9]. This confusing result is the consequence of neglecting the residual energy resolution in Ref. [5] and the contribution of the non-THM reaction mechanisms at  $\gtrsim 400$  keV. We have demonstrated above that the fit to the THM data can be done using the experimental ratio of the transfer amplitudes in the region  $\lesssim 400$  keV.

In conclusion, we recommend  $S(0) = 73.0 \pm 5.0$  MeV b for the  ${}^{15}\text{N}(p, \alpha){}^{12}\text{C}$  reaction as the result of the new fit of the R32 data from Ref. [4], which has smaller  $\chi^2/N$  than the fit to the R71 data and which overlaps with the THM result [1] and with Barker's fit if uncertainties are included.

This work was supported by the US Department of Energy under Grant Nos. DE-FG02-93ER40773 and DE-FG52-06NA26207 and NSF Grant No. PHY-0852653. We thank the late Dr. Fred Barker for stimulating discussions.

- 
- [1] M. La Cognata *et al.*, Phys. Rev. C **76**, 065804 (2007).  
 [2] J. L. Zyskind and P. D. Parker, Nucl. Phys. **A320**, 404 (1979).  
 [3] A. Schardt *et al.*, Phys. Rev. **86**, 527 (1952).  
 [4] A. Redder *et al.*, Z. Phys. A **305**, 325 (1982).  
 [5] F. C. Barker, Phys. Rev. C **78**, 044611 (2008).

- [6] C. Angulo *et al.*, Nucl. Phys. **A656**, 3 (1999).  
 [7] E. G. Adelberger *et al.*, Rev. Mod. Phys. **70**, 1265 (1998).  
 [8] A. M. Mukhamedzhanov *et al.*, J. Phys. G: Nucl. Part. Phys. **35**, 014016 (2008).  
 [9] W. Bohne *et al.*, Nucl. Phys. **A196**, 41 (1972).